

# Transformation of polarons into magnetopolarons in GaAs quantum well.

V.G. Popov<sup>a,b,\*</sup>, V.G. Krishtop<sup>a,b</sup>, M. Henini<sup>c</sup>, J.-C. Portal<sup>d,e,f</sup>

<sup>a</sup>*JSC Infotecs, Center of Scientific and Perspective Development, Stariy Petrovsko-Razumovskiy proezd 23/1, b-g 1, Moscow, 127287, Russia.*

<sup>b</sup>*Institute of Microelectronics Technology of RAS, Chernogolovka, Moscow region, 142432, Russia.*

<sup>c</sup>*School of Physics and Astronomy of Nottingham University, Nottingham, NG7 2RD, UK.*

<sup>d</sup>*GHMFL, CNRS, BP 166, F-38042, Grenoble Cedex 9, France.*

<sup>e</sup>*INSA, 135 Avenue de Rangueil, F-31077, Toulouse Cedex 4, France.*

<sup>f</sup>*Institut Universitaire de France, 103 Bd. St. Michel, F-75005, Paris, France.*

---

## Abstract

An experimental study is made of electron tunneling in a resonant-tunneling diode in magnetic fields directed parallel and perpendicular to the planes of the GaAs/Al<sub>X</sub>Ga<sub>1-X</sub>As heterostructure layers. In particular, phonon replicas on the current-voltage characteristics of the diode are investigated. In the second current derivatives a fine structure of replicas is found. The transformation of the structure of replicas in a perpendicular magnetic field can be qualitatively understood as a manifestation of the transition of polaron states to magnetopolaronic ones.

*Keywords:* quantum well, heterostructures, resonant-tunneling diodes

---

## 1. INTRODUCTION

It is well known that electrons in solids cause local deformation of the crystal lattice, forming the so-called polarons [1]. Physics of polarons is nontrivial and penetrates in all fields of the modern condensed-matter physics. To emphasize this, it suffices to mention that the ones discovered by L.D. Landau [2] polarons attracted the attention of H. Frohlich [3], J. Bardeen [4], R.P. Feynman [5]. Polarons are relevant for such effects as the colossal magnetoresistance [6] and the high- $T_c$  superconductivity [7], which are characteristic of layered crystals with two-dimensional carrier systems. Here we present

---

\*Corresponding author

*Email address:* sokhatiy@gmail.com (V.G. Popov)

*Preprint submitted to Elsevier*

*November 29, 2021*

the results of tunneling spectroscopy of polarons formed in the quantum well (QW) of a polar semiconductor.

QW polarons are usually observed in cyclotron resonance in high magnetic fields in QWs with relatively low electron concentrations [8]. Strictly speaking, this is a special type of polaron - magnetopolaron. In this case, the cyclotron energy is close to the LO-phonon energy. Polarons were also observed in tunneling spectra of QWs at zero magnetic field [9, 10]. In addition, the electron-phonon interaction was assumed to manifest itself as electron tunneling assisted by LO-phonons emission (LOPAT) or inelastic tunneling of electrons emitting the LO-phonons [11]. In fact, some features were observed in the form of additional current peaks or replicas in the  $I - V$  curves of resonant-tunnelling diodes (RTD). According to the LOPAT model, the voltage positions of the replicas should differ from the resonance peak voltage by values corresponding to the LO-phonon energy. Usually observed replicas have voltage positions very close to LOPAT, but not all, and other explanations have been suggested [12]. Moreover, the amplitudes of the replicas were usually significantly higher than the theoretical expectations. Thus, there is no good agreement between the LOPAT model and experiments.

In Ref. [13], magneto-tunnelling spectroscopy was developed to study electron dispersion in QWs. This method was applied to study phonon replicas in Ref. [10]. In particular, anti-crossing of the main resonance peak with its phonon replicas is observed. This anti-crossing can be associated with that in the polaron spectrum at the LO-phonon energy. This interpretation means the polaron origin of the peak replicas. A successful explanation of all the features was obtained by considering resonant polaron tunneling (RTP) between polaron subbands.

Here, we focus on phonon replicas in a magnetic field perpendicular to the layers of the RTD QWs. Assuming the polaron origin of the replicas, we can expect the discovery of specific features of the transformation of polarons into magnetopolarons. This transformation is accompanied by Landau quantization and charge transfer from or in the emitter QW, which is in thermodynamic equilibrium with the adjacent heavily doped GaAs contact layer [14]. In particular, there are rather wide ranges of the magnetic field in which the upper populated Landau level (LL) is attached to the Fermi level in the sense that its energy change is compensated by a change in the QW potential due to

charge transfer from or to the QW [15]. This causes a nonmonotonic shift of the current peaks in the I-V curves of the diodes [16, 17]. This inevitably affects the energy of the subband, in particular, the change in the Fermi energy in quantum wells, and should also change the energies of polaron states. As for the magnetopolarons, their energy is determined by the energy of partially filled LL, which are pinned to the Fermi levels. This indicates a weak magnetic dependence of the voltage positions of the replicas originated from the magnetopolarons. This behavior has been observed and discussed in this paper.

In Section 2 details of experiment are described, including sample and setup. In Section 3 we discuss and compare experimental data processing and theoretical predictions. The Section 4 consists of the paper conclusions.

## 2. Experiment

The investigated tunneling diodes are fabricated on the basis of an asymmetric double-barrier heterostructure. The sequence of the structure layers is shown in Table 1.

Table 1: Layer sequence of the heterostructure under investigation.

Num	Layer	Composition	Doping levels, $\text{cm}^{-3}$	Thickness, nm
1	top contact	GaAs	$2 \times 10^{18}$	500
2		GaAs	$1 \times 10^{17}$	50
3	spacer	GaAs	$1 \times 10^{16}$	50
4		GaAs	undoped	3.3
5	thin barrier	$\text{Al}_{0.4}\text{Ga}_{0.6}\text{As}$	undoped	8.3
6	well	GaAs	undoped	5.8
7	thick barrier	$\text{Al}_{0.4}\text{Ga}_{0.6}\text{As}$	undoped	11.1
8		GaAs	undoped	3.3
9	spacer	GaAs	$1 \times 10^{16}$	50
10		GaAs	$1 \times 10^{17}$	50
11		GaAs	$2 \times 10^{18}$	2000
$n^+$ - GaAs substrate				

Briefly, the GaAs QW layer is 5.6 nm thick and was grown between  $\text{Al}_{0.4}\text{Ga}_{0.6}\text{As}$

barrier layers with thicknesses of 11 and 8.3 nm. The barriers are separated from the heavily doped GaAs layers by 3.3 nm thin undoped layers and low-doped spacers, i.e. 50 nm thick GaAs layers. Diodes were fabricated from the heterostructure by the conventional methods of wet etching, photolithography, and contact annealing. Figure 1 shows the current-voltage characteristics or I-V curves of a diode with a zero and 7.5 T magnetic field directed perpendicular to the layers. The polarity of the bias voltage is chosen so that the thicker barrier is on the emitter side (see inset (a) in Fig. 1). In this case, a build-in charge in the QW is minimal. The measurements were carried out at two different temperatures. The current-voltage characteristics in a planar magnetic field were measured at  $T = 4.2$  K. The data in a perpendicular magnetic field were obtained at a temperature of 0.4 K. The current-voltage characteristics were measured for diodes with different mesa diameters range from 5 to 200  $\mu\text{m}$ .

The main current peak at  $V = V_p = 0.276$  V corresponds to the main resonance when the ground subband levels are aligned, that is,  $E_{01}(V_p) = E_{02}(V_p)$ . Inset (b) shows in more detail the peak splitting current or LO-phonon replica. In the LOPAT model, two additional peaks are associated with the emission of LO-phonons with energies  $\varepsilon_{1,2}$ .<sup>1</sup> And the voltage positions of the replica peaks  $V_{L1,2}$  are determined from the following equation:

$$V_{L1,2} = V_p + \alpha\varepsilon_{1,2}/e. \quad (1)$$

Here  $\alpha$  and  $e$  are a leverage factor and an absolute value of electron charge accordingly. In its turn the RTP model predicts other voltage positions of the replicas  $V_{R1,2}$  in accordance with following equation:

$$V_{R1,2} = V_p + \alpha(\varepsilon_{1,2} - E_{F1}(V_{R1,2}))/e \quad (2)$$

where  $E_{F1}(V_{R1,2})$  is an emitter Fermi energy in the QW with the subband level  $E_{01}$  at bias voltages  $V_{R1,2}$ . It is worth to note that RTP model can also explain features

---

<sup>1</sup>Since the quantum well is adjacent to the heterointerface, electrons interact with two types of LO-phonons. One type is in GaAs with an energy of  $\varepsilon_1 = 36$  meV, and the other lives in barrier layers with an energy of  $\varepsilon_2 = 51$  meV. Localized modes of LO-phonons can also be considered, but their energies are slightly different from bulk values, and the strength of its interaction with electrons is noticeable for narrow QW [18].

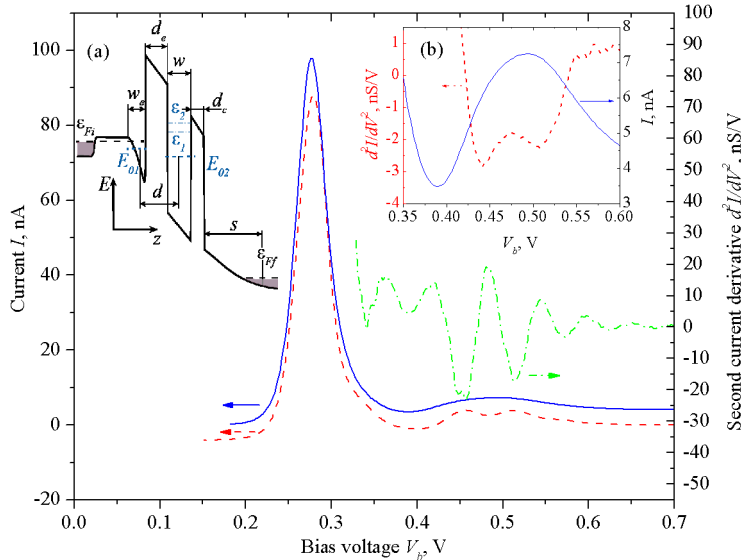


Figure 1: Tunneling characteristics of the diode. Current-voltage characteristics at zero field and a magnetic field of 7.5 T are shown by solid and dashed lines, respectively. The dashed curve is shifted on -4 nA for clarity. The second current derivative is shown by a dotted-dashed line with a 7.5 T magnetic field directed perpendicular to the layers of the heterostructure. In inset (a), the conduction band profile of the heterostructure is shown by a solid line, and the subband and Fermi levels are shown by dashed lines. The energy levels of LO-phonons are shown by dotted-dashed lines. Inset (b) shows the phonon replicas in detail as a broadened current peak (solid line) and two minima in the second derivative of the current (dashed line).

at  $V_{L,2}$  that we shall discuss in the Section 3. The key parameters to compare the models are the leverage factor  $\alpha$  and the Fermi energy in the emitter QW  $E_{F1}(V_{R1,2})$ .

These values can be obtained from examining the voltage position, i.e.,  $V_p$ , and the broadening of the main peak in the in-plane magnetic field. Figure 2 shows the I-V curves of the diode at different values of the field. In a sufficiently high field, the broadening and shift of the main current peak interact with phonon replicas, the position of which is practically insensitive to the field. A similar interaction of phonon replicas with a resonance peak was observed earlier [10] and, as mentioned above, is a consequence of anti-crossing in the polaron spectra. As far as we know, there is no theory that takes into account the polaron and in-plane field effects in the RTD. There is a theory that does not take into account polaron effects, and it takes into account the initial, final [19] and maximum [10] positions of the resonance. These experimental positions are indicated by symbols in the inset to Fig. 2. In this case, the start and end positions are determined

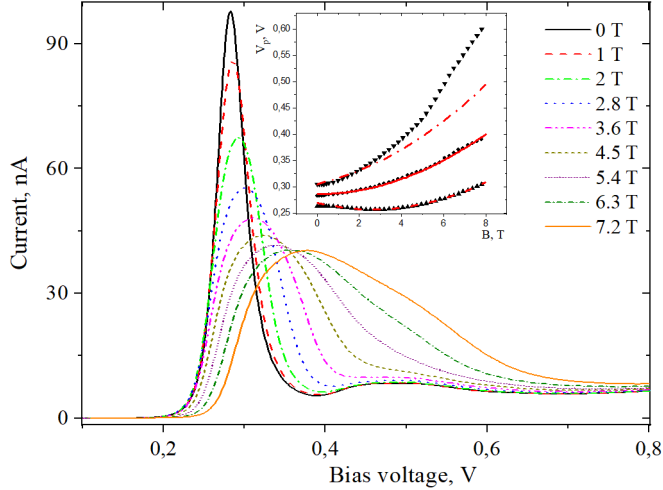


Figure 2: Current-voltage characteristics of RTDs in various in-plane magnetic fields. In the inset, the experimental positions of the beginning, end, and peak in the resonance are shown by triangles with vertices up, down, and circles respectively. The best-fitted calculated values of the beginning  $V_s$ , end  $V_f$ , and position of the resonance peak  $V_p$  are shown by dashed, dash-dotted, and solid lines, accordingly.

as the voltages at which the current is at half the peak value, measured relative to the current "valley" on either side of the current peak. The lines show the calculated best-fit values. A good match of the start and peak positions is seen. From this fit, you can extract the  $E_{F1}$  and the leverage factor using the method described in the next section. In particular, the best-fitted value for  $E_{F1}(V_p)$  is 2.5 meV.

The most significant result was observed in a magnetic field directed perpendicular to the plane of the QW. First of all, additional features appeared on the I - V curve, which are more clearly observed in the second derivative of the current, as can be seen in Fig.1. The voltage position of these features depends on the field. These features are associated with tunneling between LLs with different indices, which is facilitated by the emission of LO-phonons [20]. The field dependences of the features will be discussed elsewhere. Here, the main attention is paid to the transformation of phonon replicas in a perpendicular magnetic field. In Fig. 3, the second current derivatives are plotted in the voltage range of the phonon replica at different perpendicular magnetic fields. First of all, one can see a significant increase in the amplitudes of the replicas. Secondly, the replica

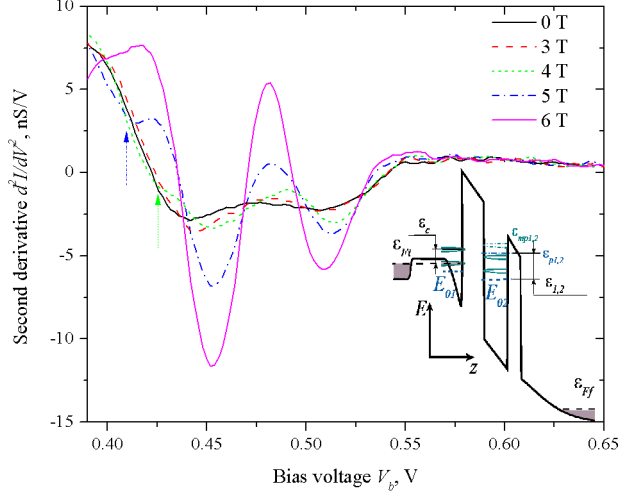


Figure 3: Second current derivative versus bias voltage at different perpendicular magnetic fields. In the inset the conduction-bottom profile of the RTD is plotted as solid line with quantum levels.

at  $V_b = 0.45$  V is split into two, one noticeably shifts with increasing field towards a lower voltage, and the other is formed at a higher voltage, which is practically insensitive to the field. The position of the feature at  $V_b = 0.53$  V is slightly sensitive to the field. In this case, its amplitude decreases and a new feature appears at a higher voltage. This behavior is hardly understandable in the LOPAT model, and we will discuss it in the RTP model.

### 3. Discussion

First off all let's consider the electron spectrum as parabolic one at zero magnetic field as follows:

$$\varepsilon(p) = p^2/2m_* \quad (3)$$

where  $p$  is an 2D electron momentum,  $m_*$  is an electron effective mass. According to Eqs (1, 2), we can expect phonon replicas to be at lower voltages than in the LOPAT model. The difference in voltage positions is determined by the Fermi energy in the emitter QW. The Fermi energy of the emitter and the leverage factor can be found

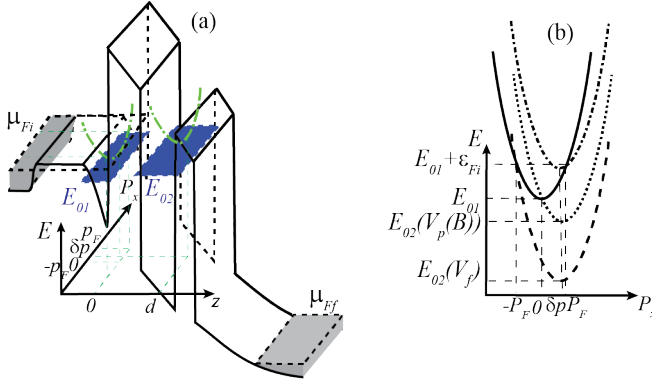


Figure 4: Bottom profile of the conduction band of the heterostructure under investigation with quantum levels and dispersion curves (a). Intersection of the dispersion parabolas of the QWs at different bias voltages (b). Intersection of the solid and dotted curves takes place at  $V = V_p$ , that of the solid and dot-dashed curves at  $V_s$  and that of the solid and dashed curves at  $V_f$ .

from the behavior of the peak of the resonant current in a in-plane magnetic field (see Fig. 2). In the field, the resonance broadens, which can be understood in the model of sequential electron tunneling between QWs with the  $E_{01}$  and  $E_{02}$  levels. In this case, the tunneling conserves the generalized electron momentum  $P_x = p_x + eA_x$  instead of the usual momentum  $p_x$  [21]. Assuming a weak field, one can consider the common vector potential for all electrons in QWs [19] as follows:  $A_x = eB \langle z \rangle$ . Here, the vector potential  $A_x$  is in the Landau gauge for a magnetic field directed in the direction  $y$ , i.e.  $\mathbf{B} = (0, B, 0)$  and  $\langle z \rangle$  is the mean position of electrons in the QW along the  $z$  axis. To demonstrate the effect of the field, it is convenient to consider the electronic spectra as a function of  $P_x$  (see Fig. 4(a)). To participate in coherent tunneling, an electron must conserve its energy and generalized momentum. This means that coherent electron tunneling can occur in the electronic state, which is defined as the intersection point of the dispersion curves (see Fig. 4(b)).

Coherent tunneling begins and ends when the intersection point coincides with the Fermi level in the emitter, which corresponds to the intersection of the dash-dotted and dashed curves, respectively, with solid one in Fig. 4(b). From this picture, you can get the equations for the energy of the  $E_{01,2}$  levels as follows:  $E_{01}(V_s) + \varepsilon_{Fi} = E_{02}(V_s) + \varepsilon(P_F - \delta p)$ . Where  $V_s$  is the voltage of the start of coherent tunneling, and  $\delta p = e\delta A_x = eBd$ ,  $d = \delta z = \langle z_2 - z_1 \rangle$  is the average distance between electrons in the  $z$ -direction in

the emitter and inter-barrier QWs. Similar conditions for the voltage  $V_f$  of the finish of coherent tunneling can be written as follows:  $E_{01}(V_f) + \varepsilon_{Fi} = E_{02}(V_f) + \varepsilon(P_F + \delta p)$ . From the definition of the leverage factor  $\alpha$  you can get the following equation:  $e(V - V_p) = \alpha(E_{01}(V) - E_{02}(V))$ . Therefore, the following equations for the start and finish voltages can be obtained:

$$V_{s,f}(B) = V_p(0) + e^{-1}\alpha(\varepsilon(P_F \pm eBd) - \varepsilon_{Fi}) \quad (4)$$

Here  $V_p(0)$  corresponds to the resonant voltage at zero field. As for the finite field  $V_p(B)$  can be determined from intersection of the solid and dotted curves (see Fig. 4(b)) in similar way as Eq. (4) [10] as follows:

$$V_p(B) = V_p(0) + e^{-1}\alpha\varepsilon(eBd) \quad (5)$$

From fitting the dependencies in the Eq. (4, 5) to the experimental values, we can extract the values of  $\varepsilon_{Fi}$  and  $\alpha$ . The best curves are shown in the inset to Fig. 2. It should be noted that the fit was performed for the current peak and start of resonance voltages, i.e.  $V_p$  and  $V_s$ , which are shown by circles and upper triangles, respectively. The values  $\alpha = 4.8$  and  $E_{F1}(V_p) = 2.5$  meV are extracted from the parameters of the curves. Extract details are discussed in Appendix. Using these parameters, one can also calculate voltages of the resonance finish  $V_f$ , shown by the dashed curve in Fig. 2. A noticeable discrepancy is seen between the calculated and experimental data of  $V_f$  in high magnetic fields. This discrepancy is a consequence of the nonparabolic spectrum at energies close to LO-phonon energy, that is, the polaron effect.

To clarify the difference between the LOPAT model and the RTP, it is worth discussing the polaron subbands. According to the RTP model [10], polaron subbands are formed in the electron and LO-phonon spectra in zero magnetic field. Here we call the polaron subband the one in which the polarons are formed by real LO-phonons. Strictly speaking, the spectrum of polarons is split in the LO-phonon energy into two branches or subbands. The splitting is the result of anti-crossing caused by electron-phonon interaction. The low-energy branch corresponds to polarons formed by virtual LO-phonons, and the upper-energy branch is associated with real LO-phonons. In this case, the bottoms of the polaron subbands over-top the subband level at LO-phonon energies. In the

heterostructure, the LO-phonon spectra are different for layers of different compositions, and all LO-phonons interact with electrons. In particular, the structure under investigation contains two types of LO-phonons with energies  $\varepsilon_1 = 36$  meV (in GaAs layers) and  $\varepsilon_2 = 51$  meV (in AlGaAs layers). The effective mass of polarons is practically infinite at a small momentum in the polaron subband. Considering the direct resonant tunneling of electrons or polarons of lower mass into the polaron subband, one can easily conclude that the number of resonant states or the resonant current is maximum when the bottom of the polaron subband is aligned with the Fermi energy in the emitter 2DEG. This gives the Eq. (2) for the replicas voltage positions.

As noted above, phonon replicas can be explained by the manifestation of inelastic electron tunneling. In this case, the electron can decrease its energy by emitting an LO-phonon during tunneling in the QW. This is LO-phonon assisted tunneling (LOPAT) [11]. The LOPAT theory predicts that electrons mainly emit LO-phonons with low lateral momentum components. This means that the lateral momentum of the electron is practically conserved in the model. This provides LOPAT current peaks when the applied voltage shifts the level of the  $E_{02}$  subband of the quantum well below the level of the emitter subband  $E_{01}$  at the LO-phonon energy  $\varepsilon_{1,2}$ . At the same time, RTP should start at a lower voltage than LOPAT, and this difference should depend on the concentration of electrons in the emitter [10]. In this case, the voltage replica positions are given by equation (1).

The best-fit parameters enable us to compare the LOPAT and RTP models when predicting the position of phonon replicas. Having determined the voltage positions of the dips in the second current derivatives at zero field as  $V_{p1} = 0.44$  V and  $V_{p2} = 0.508$  V, we can calculate the corresponding energies as  $\varepsilon_{p1} = e(V_{p1} - V_p)/\alpha = 34.2$  meV and  $\varepsilon_{p2} = e(V_{p2} - V_p)/\alpha = 48.3$  meV. The values are less than the energy of LO-phonons, but taking into account the Eq. (2) and the Fermi energy of the emitter, we can obtain the following:  $\varepsilon_1 = \varepsilon_{p1} + \varepsilon_{Fi} = 36.9$  meV and  $\varepsilon_2 = \varepsilon_{p2} + \varepsilon_{Fi} = 51$  meV, which exactly coincides with the energies of LO-phonons in GaAs and AlGaAs. This gives us strong support for the RTP model, but what the model can explain for data obtained in a perpendicular magnetic field .

In the high enough perpendicular magnetic field the electron spectrum is strongly

quantized and LLs are well resolved. In this case the LLs are split on cyclotron energy  $\varepsilon_c = eB/m_*$  and over-topped the subband energy  $E_{01,2}$  of the QWs in accordance with Landau equation:

$$E_{LL} = E_{01,2} + (i + 1/2)\varepsilon_c \pm \mu B \quad (6)$$

Here  $i$  is the LL index,  $E_{LL}$  is the LL energy,  $\mu$  is the Bohr magneton. The Landau equation is derived for free charged particles and can only be used for polarons with a weak electron-phonon interaction or polarons of the low-energy branch. In the case of high-energy subbands, from a theoretical point of view, the polaron energy is simply determined by the energy of low-energy polarons, shifted by the energies of LO-phonons insensitive to the magnetic field [22]. This simple picture does not take into account the conditions for detecting of Landau levels. The condition is as follows: the magnetic length  $l_m$  must be less than the localization length of polarons  $l_l$ . In the case of high-energy polarons produced by real LO-phonons,  $l_m$  is not a well-defined parameter, since the polaron charge  $q$  is determined by the electron-phonon interaction and is less than  $e$ . This means that the polaron  $l_m$  is longer than the electron one, because  $l_m = \sqrt{\hbar/qB}$ . Also a good question is what is the localization length of the polaron. Probably the length of  $l_l$  is proportional to the phonon wavelength  $\lambda_p$ . Due to the weak dispersion of LO-phonons,  $\lambda_p$  takes on a very wide range of values. Thus, one can expect a fairly wide range of  $B$  for the conversion of polarons to magnetopolarons. And this range is determined by such little-known parameters of the polarons like  $l_m$  and  $l_l$ .

The observation of the transition of polarons to magnetopolaron states is accompanied by such an effect as LL pinning. Let us consider it in more detail. By changing the magnetic field  $B$ , one can change  $\varepsilon_c$ ,  $E_{LL}$  and the number of filled LL. This change can self-consistently lead to the pinning of the upper LL at the Fermi levels of the adjacent contacts. From the Fermi energy of the emitter, it can be obtained that for a field  $B > 2$  T, the filling factor LL is less than 2. This means that the lowest LL is fixed by the Fermi level in the emitter, and the magnetic field shifts the level of the subband  $E_{01}$  in accordance with the Eq. (6).

In this case, since high-energy polaron subbands are formed at energies close to the energies of LO-phonons, overtopped the level of the subband or the bottom of the conduction band, they will be sensitive to the field. In particular, the bottom of the conduction

band and the polaron mediated by electrons with the subband level  $E_{02}$  should decrease with increasing field (see  $\varepsilon_{p1,2}$  in the inset to Fig. 3). This behavior is observed in Fig. 3 for the features indicated by the arrows. However, there are high amplitude features, the voltage position of which is almost insensitive to the field. They are characterized by an increase in amplitude with increasing field. To explain them, it is necessary to consider the states of the magnetopolaron, which are formed from the electronic states LL. The states of the magnetopolaron exceed LL at the energies of LO-phonons  $\varepsilon_1$  and  $\varepsilon_2$  (see  $\varepsilon_{mp1,2}$  in the inset to Fig. 3). Since LL is fixed at Fermi levels, the energy of magnetopolarons is insensitive to the field. As for the amplitude, it grows with the field due to an increase in the LL degeneracy. The replica positions can be found as the dip positions in the second current derivative (see Fig. 3) as follows:  $V_{mp1} = 0.452$  V and  $V_{mp2} = 0.510$  V. Using the leverage factor, the corresponding energy can be determined as follows:  $\varepsilon_{mp1} = e(V_{mp1} - V_p)/\alpha = 37$  meV,  $\varepsilon_{mp2} = e(V_{mp2} - V_p)/\alpha = 48.8$  meV. These values are very close to the energy of LO-phonons in GaAs  $\varepsilon_1 = 36$  meV and AlGaAs  $\varepsilon_2 = 51$  meV, but they are not as accurate as the data obtained in planar magnetic fields. A perpendicular magnetic field dramatically changes the spectrum of electrons, as well as in the state of magnetopolarons, and a change in the leverage factor is quite expected. However, within the framework of the RTP model, the behavior of phonon replicas is qualitatively clear.

#### 4. Conclusion

Summing up, it can be argued that detailed experimental studies of phonon replicas in magnetic fields of different orientations were carried out for the first time. The leverage factor and the Fermi energy of the emitter were extracted from the I - V characteristic of the diode in an in-plane field, which allows us to compare the voltage positions of phonon replicas predicted by different theoretical models. The RTP model is more suitable for describing experimental data. In a perpendicular magnetic field, a transformation of phonon replicas was observed, which can be qualitatively described as the transformation of polarons into magnetopolarons, accompanied by LL pinning.

## Appendix

Strictly speaking, the fitting of the calculated data (see Fig. 2) was carried out by varying two parameters  $a$  and  $b$  of the following parabolas:

$$V_p(B) = V_p(0) + a \times B^2 \quad (7)$$

$$V_s(B) = V_s(0) - b \times B + a \times B^2 \quad (8)$$

The best-fit values of  $a$  and  $b$  are 1.8 mV/T<sup>2</sup> and 9.3 mV/T accordingly. From Eqs. (4, 5) one can find the values as follows:

$$a = \alpha e d^2 / 2m_* \quad (9)$$

$$b = \alpha d P_F / m_* \quad (10)$$

Thus, using the two best-fitted parameters, we have to determine three unknown values  $\alpha$ ,  $d$  and  $P_F$ . Obviously, the third equation is necessary and can be found by considering the leverage factor in detail.

The leverage factor can be estimated using the Stark effect approximation. In this case, the levels  $E_{01}$  and  $E_{02}$  change their energy in accordance with the electric field  $F$  as follows  $E_{01,2}(F) = E_{01,2}(0) + eFz_{1,2}$ , where  $z_{1,2}$  are the average positions of electrons in quantum wells. Therefore, the level difference can be found as follows:

$$\Delta E_{1,2}(F) = E_{01}(F) - E_{02}(F) = \Delta E_{1,2}(0) + eF(z_2 - z_1) = \Delta E_{1,2}(0) + eFd \quad (11)$$

Suppose that the electric field  $F$  is homogeneous in the active region of the diode (see inset (a) in Fig. 1), we can express the field value as follows:

$$F = V / (w_e + d_e + w + d_c + s) \quad (12)$$

Here the  $w_e$  is a width of the emitter QW or accumulation layer,  $d_e$  is a thickness of the emitter barrier,  $w$  is a width of the inter-barrier QW,  $d_c$  is a collector barrier width

and  $s$  is a collector spacer width (see Fig. 1). Combining the Eqs. (11) and (12) one can deduce the following:

$$\Delta E_{1,2}(V) = \Delta E_{1,2}(0) + eVd/(w_e + d_e + w + d_c + s) \quad (13)$$

According Eq. (13) the leverage factor can be found as follows:

$$\alpha = \frac{e}{d\Delta E_{12}/dV} = \frac{w_e + d_e + w + d_c + s}{d} \quad (14)$$

The tunnel distance  $d$  can be roughly estimate as follows:

$$d = d_e + (w_e + w)/2 \quad (15)$$

All lengths are well defined by the layer width, with the exception of the  $w_e$  accumulation layer width. Calculation of  $w_e$  goes beyond the uniform-electric-field approximation and requires self-consistent calculations of the Poisson and Schrödinger equations. In any case, using the Eqs (14, 15, 9, 10) one can outdraw the value  $w_e = 5.6$  nm, which corresponds to the leverage factor  $\alpha = 4.8$ . From Eq. (10) taking into account that  $P_F = p_F = \sqrt{2m_*E_{F1}}$  one can calculate the emitter Fermi energy as follows:  $E_{F1}(V_p) = 2.5$  meV.

## References

- [1] J. T. Devreese, *Polarons in Ionic Crystals and Polar Semiconductors* (North-Holland, Amsterdam, 1972).
- [2] L.D. Landau, *Sov. Phys.* **3**, 664 (1933).
- [3] H. Fröhlich, *Adv. in Phys.* **3**, 325 (1954).
- [4] J. Bardeen and W. Shockley, *Phys. Rev.* **80**, 72 (1950).
- [5] R.P. Feynman, R.W. Hellwarth, C.K. Iddings and P.M. Platzman, *Phys. Rev.* **127**, 1004 (1962).
- [6] M. Jaime, H.T. Hardner, M.B. Salamon, M. Rubinstein, P. Dorsey and D. Emin, *Phys. Rev. Lett.* **78**, 951 (1997).
- [7] *Lattice Effects in High-Tc Superconductors*, edited by Y. Bar-Yam, T. Egami, J. Mustre de Leon, and A. R. Bishop. (World Scientific, Singapore), 1992.
- [8] H. Sigg, P. Wyder and J.A.A.J. Perenboom, *Phys. Rev. B* **31**, 5253 (1985).
- [9] I.N. Kotelnikov, S.E. Dizhur, *JETP Letters*, **81**, 574 (2005).
- [10] V.G. Popov, V.G. Krishtop, O.N. Makarovskii, and M. Henini, *JETP*, **111**, 220 (2010).
- [11] H. Mizuta and T. Tanoue, *The Physics and Applications of Resonant Tunneling Diodes* (Cambridge Univ. Press, Cambridge), 53, 1995.
- [12] K. Kempa, E. Gornik, K. Unterrainer, M. Kast, G. Strasser, *Phys. Rev. Lett.* **86**, 2850 (2001).
- [13] R.K. Hayden, D.K. Maude, L. Eaves, E.C. Valadares, M. Henini, F.W. Sheard, O.H. Hughes, J.C. Portal, *L. Cury. Phys. Rev. Lett.* **66**, 1749 (1991).
- [14] K. S. Chan, F. W. Sheard, G. A. Toombs, L. Eaves, *Phys. Rev. B* **56**, 1447 (1997).
- [15] V.G. Popov, *Phys. Rev. B* **73**, 125310 (2006).
- [16] V.G. Popov, Yu.V. Dubrovskii, J.C. Portal, *JETP*, **102**, p. 677 (2006).
- [17] V.G. Popov, O.N. Makarovskiy, V.T. Renard, J.-C. Portal, *Physica E*, **43**, 151 (2010).
- [18] M.A. Stroscio, M. Dutta *Phonons in Nanostructures*, (Cambridge: Cambridge University Press) 131, (2004).
- [19] W. Demmerle, J. Smoliner, G. Berthold, E. Gornik, G. Weimann, W. Schlapp, *Phys. Rev. B* **44**, 3090 (1991).
- [20] M.L. Leadbeater, E.S. Alves, L. Eaves, M. Henini, O.H. Hughes, A. Celeste, J.C. Portal, G. Hill, and M. A. Pate, *Phys. Rev. B* **39**, 3438 (1989).
- [21] L.D. Landau, E.M. Lifshitz *Theoretical physics. Quantum mechanics. Non relativistic theory.* v 3, p. 523 (Fizmatlit, Moscow, 1973).
- [22] J. T. Devreese, *Encyclopedia of Applied Physics*, Vol. 14, pp. 383-409 (1996).